3-9

A New Comprehensive and Experimentally Verified Electron Transport Model for Strained SiGe

F. M. Bufler, P. Graf, and B. Meinerzhagen
Institut für Theoretische Elektrotechnik und Mikroelektronik, Universität Bremen, D-28334 Bremen, Germany
Phone: +49 421-218 2204 Fax: +49 421-218 4434
H. Kibbel
Daimler-Benz AG, Research Center Ulm, D-89013 Ulm, Germany
G. Fischer
Institut für Halbleiterphysik, PSF 409, D-15204 Frankfurt (Oder), Germany

The favorable properties of Si/SiGe heterojunction bipolar transistors (HBT's) for applications in the GHz range and the possibility to integrate these devices together with silicon CMOS circuitry on one chip will lead to a replacement of GaAs based components by SiGe based parts for many high frequency applications in near future. Hence there is an increasing demand for an accurate modeling of carrier transport in strained SiGe. But despite this apparent importance all electron transport models for strained SiGe published so far are of limited generality (e.g. neglect nonparabolicity and the influence of Ge on phonon scattering [1, 2, 3]) and are not verified experimentally by measurements of ohmic mobility in strained SiGe layers. This paper aims at closing this gap.

Within the new model the conduction band structure of strained $Si_{1-x}Ge_x$ ($x \leq 0.75$) grown on a (001)-Si substrate is described by six ellipsoidal and nonparabolic valleys [4], two of which are shifted upwards in energy under the biaxial compressive strain. The valley shifts and the effective masses are modeled as a function of relative Ge content x as described in [5, 6]. The nonparabolicity is set to α=0.44 eV^{-1} independently of x. The phonon system considers all relevant scattering processes in the Si-like band structure with its six valleys along the Δ lines as reported in [4] for Si. Phonon energies determining the thresholds for optical phonon emission are distinctly different in Si and Ge. This effect is taken into account by considering the phonon scattering rates of both Si and Ge linearly weighted by their relative fraction in the alloy. The Ge phonon energies for interband scattering between the valleys on the Δ axes are extracted from the phonon dispersion relation of Ge. Essentially the same values as in Si are taken for the corresponding coupling constants. Alloy scattering is modeled according to [7] considering both intravalley and intervalley scattering. The unknown scattering potential was chosen such that the experimental data of [8] for relaxed SiGe are reproduced between $x = 0.3$ and $x = 0.6$ where the data are least noisy (see Fig. 1). From a theoretical standpoint the proper modeling of impurity scattering is still a controversial issue. On the other hand reliable experimental data for ohmic majority and minority electron mobility as a function of doping is readily available in Si. Therefore as an engineering compromise the ionized impurity scattering model of Ridley [9] is adopted with a doping dependent adjustment to mobility measurements (see Fig. 2) to account for all additional effects like degeneracy etc. (Please note that majority carrier drift mobility is extracted from resistivity under the assumption of complete ionization). In SiGe the only additional modification of the Ridley model consists of a linear interpolation of the dielectric constant between its respective values in Si and Ge. Hence all scattering model parameters of the transport model presented here have been derived exclusively from available literature data on unstrained Si, Ge or SiGe.

In order to allow an independent experimental verification of the model for strained SiGe special test structures (see Fig. 3) were grown on a silicon substrate using molecular beam epitaxy (MBE) or low pressure chemical vapor deposition (LPCVD). Electric isolation of the antimony (MBE) or phosphorus (LPCVD) doped SiGe layer was achieved by a p-type doping of the Si substrate and the Si cap layer with a boron concentration of $N_A = 10^{16} cm^{-3}$. The resistivity in the strained SiGe layer was determined by using four-point measurements and the dopant density and Ge content was measured by secondary ion mass spectroscopy. Finally the in-plane component μ_{xx} of the drift mobility was extracted under the assumption of complete activation and ionization. Fig. 4 shows the good agreement between the results of the transport model and the experimental results proving the validity of our model for both dopants (antimony, phosphorus) and growth techniques (MBE, LPCVD).

In Fig. 5 and Fig. 6 majority and minority mobilities are displayed as a function of Ge-content for different doping levels. Our model shows only a small difference between the mobility in unstrained SiGe and the in-plane mobility component of strained SiGe. The reason is that the smaller effective mass in unstrained SiGe is balanced by the relative reduction of the alloy scattering rate in strained SiGe as a consequence of the valley shifts. The absence of this feature in [1, 2, 3] may be due to a smaller alloy scattering potential which would reduce this effect. Less alloy scattering may be as well the main reason for the higher SiGe mobilities reported in these papers.

In summary, we have presented an accurate and experimentally verified model for electron transport in strained and unstrained SiGe alloys which is also well suited for implementation into a Monte Carlo device simulator for Si/SiGe HBT's. One important result of our model for technical applications is that for the Ge contents and doping levels of highest technical interest the minority electron mobility perpendicular to the Si/SiGe interface in strained SiGe grown on Si is approximately equal to the respective mobility in unstrained Si (see Fig. 6).

Acknowledgments This work was supported by the Bundesministerium für Bildung, Wissenschaft, Forschung und Technologie under contract no. 01 M 2416 A. Discussions with P. Vogl (TU München), M. M. Rieger (University of Cambridge), D. Temmler (Institut für Halbleiterphysik Frankfurt/Oder) and U. König (Daimler-Benz Ulm) are gratefully acknowledged.

References

[1] B. Pejčinović et al., IEEE Trans. ED **36**, 2129 (1989)
[2] L. E. Kay et al., J. Appl. Phys. **70**, 1483 (1991)
[3] T. Manku et al., IEEE Trans. ED **39**, 2082 (1992)
[4] C. Jacoboni et al., Rev. Mod. Phys. **55**, 645 (1983)
[5] M. M. Rieger, master thesis, TU München, 1991
[6] M. M. Rieger et al., Phys. Rev. B **48**, 14276 (1993)
[7] J. W. Harrison et al., Phys. Rev. B **13**, 5347 (1976)
[8] G. Busch et al., Helv. Phys. Acta **33**, 437 (1960)
[9] B. K. Ridley, J. Phys. C **10**, 1589 (1977)
[10] A. B. Sproul et al., J. Appl. Phys. **72**, 4161 (1992)
[11] S. E. Swirhun et al., *IEDM Tech. Dig.*, 24 (1986)
[12] W. R. Thurber et al., J. Electrochem. Soc. **127**, 1807 (1980)

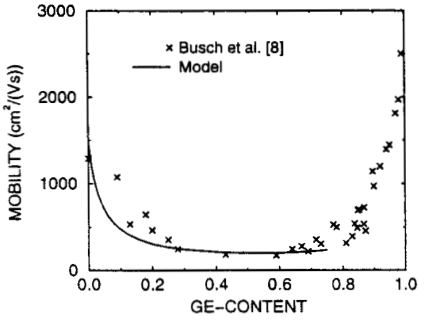

Figure 1: Experimental results [8] and theory for electron mobility in undoped and unstrained SiGe at 293 K

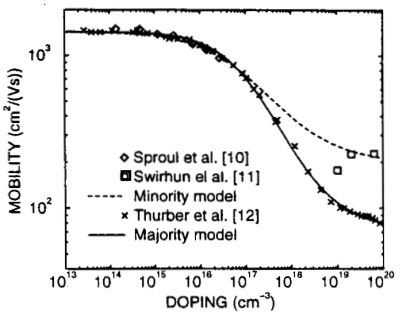

Figure 2: Electron drift mobilities in unstrained Si at 300 K in comparison to experiments for minorities [10, 11] and majorities [12]

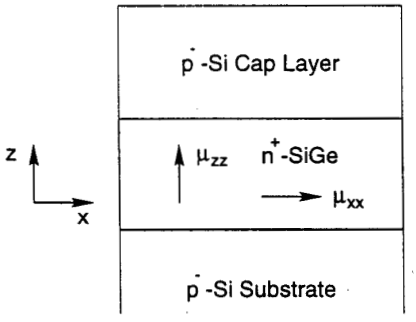

Figure 3: Simplified cross section illustrating direction of tensorial mobility components and experimental setup

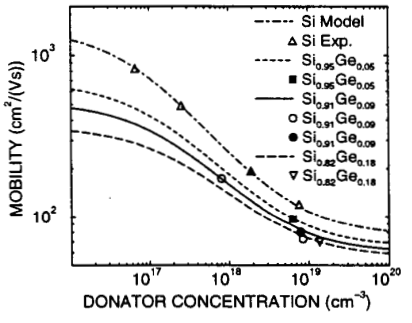

Figure 4: Experimental results and theory for in-plane component μ_{xx} of majority drift mobility in strained SiGe at 295 K (open symbols = MBE samples, filled symbols = LPCVD samples).

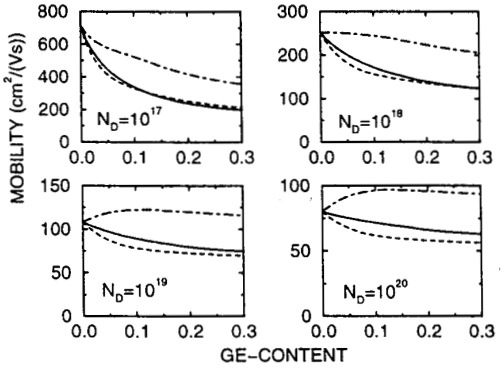

Figure 5: Majority electron mobilities of SiGe for four doping levels (in cm^{-3}) at 300 K: dot-dashed line $\equiv \mu_{zz}$ of strained SiGe, solid line $\equiv \mu$ of unstrained SiGe, dashed line $\equiv \mu_{xx}$ of strained SiGe

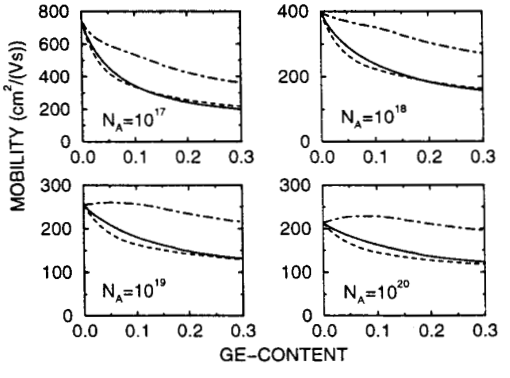

Figure 6: Minority electron mobilities of SiGe, same legend as in Fig. 5